KINEMATIC CONTROL MODES FOR TELEOPERATION OF REDUNDANT ROBOTS

Richard Hooper
The University of Texas at
Austin Robotics Research Group
Austin, Texas 78712-1100
(512)471-7098

Mark W. Noakes
Oak Ridge National Laboratory
Robotics and Process Systems Division
Oak Ridge, Tennessee 37831-6304
(423)574-5695

ABSTRACT

Nuclear facility dismantlement tasks include disassembly of process equipment, cutting pipe, size reduction of equipment, transport of materials, and decontamination of floors, walls, and remaining equipment. Plans for using robots to perform these tasks specify direct teleoperation in the near-term with a transition to more autonomous robots as the technology becomes available. As this control progresses from direct teleoperation to autonomous robots, the sophistication of the human intervention must correspondingly increase. This paper discusses different levels of interaction between a human operator and a remote redundant robot. The discussion includes development, implementation, and test results for five different modes of teleoperation. Two of these modes include a degree of computer-based decision making. Results show that the computer is capable of making very fast decisions when confronted with complex kinematic problems. The difficulty lies primarily in the computer's need for information about the location of obstacles in the robot's workplace.

I. INTRODUCTION

A spectrum of tasks in unstructured environments characterizes the Decontamination and Dismantlement (D&D) mission. Telemanipulators represent a technology for accomplishing a portion of the mission's task spectrum. Telemanipulators allow the human to project manipulative capabilities into remote hazardous environments. Giving these telemanipulators extra kinematic degrees of freedom (kinematic redundancy) enables them to perform a wider range of tasks, thus further amortizing costs. Developed by the United States Department of Energy (DOE), the Dual Arm Work Module (DAWM) is an example of a telemanipulator with kinematic redundancy. The DAWM (Figure 1.) has 17 Degrees Of Freedom (DOF) arranged in 2 serial chains each having 8 independent DOF and sharing 1 common center rotational joint. Red Zone Robotics manufactured and delivered the 5 DOF base unit that includes the common rotational joint and the next two joints in both chains. Schilling Titan II manipulators form the last six DOF for each chain. With two arms and 17 DOF, the system has 5 degrees of kinematic redundancy.

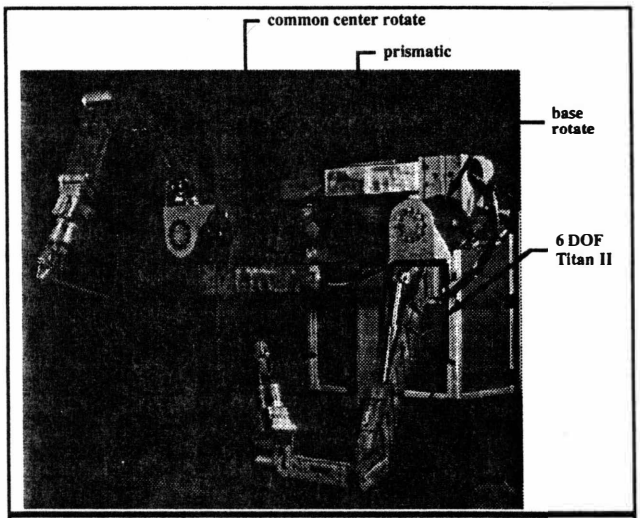

Figure 1. The Dual-Arm Work Module

This kinematic redundancy gives the system the versatility to perform a very wide range of tasks. Furthermore, the redundancy typically affords a number of different kinematic options for performing each task. In other words, the robot can move its body while holding its End-EFfectors (EEF) at constant locations. These motions represent sets of configuration options. The operator (or the robot's own internal decision-making algorithms) can choose an option best suited for a given task. A skilled operator will choose an option based on visual feedback and experience with important system parameters. These parameters represent operational performance criteria:

joint motion limits - travel, velocity, acceleration, torque
dual arm criteria - relative load, energy, compliance
obstacle avoidance - model for system and environment
task criteria - force, deformation, dexterity.

Machine-based decision-making algorithms must match or surpass this level of sophistication before they can begin to share control with human operators.

This paper discusses five control modes developed specifically for the DAWM, though they apply in general to all redundant telemanipulators. Table 1. lists these modes in an order of increasing sophistication.

Table 1. A brief description of the five control modes.

Control Mode	Brief Description
Joint-	Drive each joint independently
Decoupled Cartesian-	A six-joint subset in Cartesian, and extra joints independently
Self-Motion-	Drive individual joints while maintaining hand position
Advisor-	Computer suggests configuration based on task specifications
Coupled Cartesian-	Computer automatically controls all joints based on hand controller input and task specifications

These control modes represent steps in the hierarchy of teleoperation. Draper describes a continuum in the sophistication of the operator's interaction with the machine during teleoperation.[1] In an order of increasing sophistication, the types of control in the continuum follow as: manual control, intelligent assistance, shared control, traded control, and supervisory control. The first three modes from Table 1. are examples of manual control. The advisor mode is an intelligent assistant and the coupled-Cartesian mode is in the category of shared control.

II. MANUAL CONTROL

The lowest three control modes fall into the category of manual control. Though these control modes employ very sophisticated electronics and computer algorithms, there is no machine-based decision-making involved as the operator controls the robot's extra joints. Thus, the joint, decoupled-Cartesian, and self-motion modes of teleoperation fall into the category of manual control.

Joint control is the simplest mode. In this mode the operator drives each of the robot's joints independently. Precisely controlling the location of the robot's end-effector is very difficult in this mode. The mode is, however, very useful for extricating the robot from difficult configurations. These difficult configurations may involve joint travel limits, singularities, and workspace boundaries. In the joint control mode, the operator can simply jog each joint until the robot is in a more favorable configuration. After that, the operator can switch the control mode to a more sophisticated level of interaction.

In decoupled-Cartesian control, the operator drives the first five base axes in simple joint mode. The operator controls the last 6 axes in a traditional Cartesian mode. This is the classic DOE teleoperation. The operator is specifying as many kinematic constraints on the system as there are DOF. In this case, the operator is specifying 6 constraints for each EEF location and there are 6 DOF in each arm. Essentially, the operator is in remote control of a state-of-the-art telemanipulator.

Self-motion control allows the operator to drive each of the robot's axes in joint mode while maintaining the end-effector at a constant location. This allows the operator to optimize the robot's configuration after establishing a work point. As with decoupled-Cartesian control, the operator is specifying the same number of kinematic constraints as there are DOF in the system. Though the operator is still in remote control of the manipulator, this mode is a useful extension to the capabilities of classic DOE teleoperation.

Implementing both the decoupled-Cartesian and the self-motion modes of teleoperation requires the solving of an inverse kinematics problem. For the DAWM, the geometry of the Schilling Titan II manipulator determines the inverse problem.

Figure 2. shows a schematic of the Schilling arm. The offset at the wrist prevents the last three joint axes from intersecting at a point (no spherical wrist). This complicates the analysis somewhat. The following analysis provides a solution involving polynomials of degree 2 or less. The analysis follows three basic steps. The first step solves for Φ and θ_1 using the constraints on position (P_x, P_y, P_z) and orientation (α, β, γ). The next step uses Φ and θ_1 to remove the effects of the wrist offset. After this, step three solves for θ_2 through θ_6 as if the robot had a spherical wrist.

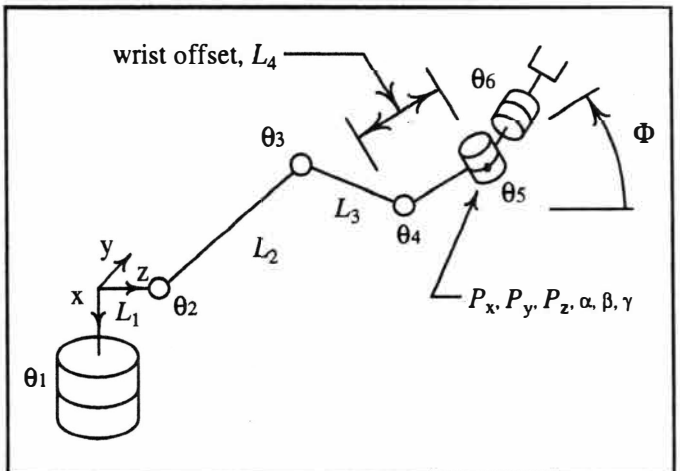

Figure 2. Schematic of the Schilling geometry

The analysis begins by finding θ_1. Since θ_2, θ_3, and θ_4 are in parallel:

$$\theta_1 = \text{a}\,tan\,2(P_y, P_z).$$

Using YXZ Euler angles to match the rotations at the wrist:

$$\begin{aligned} {}^0_6R &= R_y(\alpha)R_x(\beta)R_z(\gamma) \\ {}^0_\Phi R &= R_x(-\theta_1) \\ {}^0_6R &= {}^0_\Phi R\,{}^\Phi_6 R \\ {}^\Phi_6 R &= {}^0_\Phi R^{-1}\,{}^0_6 R. \end{aligned}$$

Extracting YXZ Euler angles from ${}^\Phi_6R$ gives:

$$\Phi = \alpha.$$

By finding Φ and θ_1, this completes the first step in the analysis.

The next step in the analysis uses Φ and θ_1, to eliminate the effects of the wrist offset, L_4, and transforms P_x, P_y, P_z into P'_x, P'_y, P'_z. The transformation proceeds as follows:

$$\begin{aligned} P'_x &= P_x - L_4 \sin\Phi \\ P'_y &= P_y - L_4 \cos\Phi \sin\theta_1 \\ P'_z &= P_z - L_4 \cos\Phi \cos\theta_1. \end{aligned}$$

This transformation essentially subtracts the effects of the offset.

Given P'_x, P'_y, P'_z, the final step in the procedure solves for the joint displacements as is the robot had a spherical wrist. The forward position solution for the transformed geometry generates the following geometric equations:

$$\begin{aligned} P'_x &= L_2 \sin\theta_2 + L_3 \sin(\theta_2 + \theta_3) \\ P'_y &= L_1 \sin\theta_1 + L_2 \sin\theta_1 \cos\theta_2 + L_3 \sin\theta_1 \cos(\theta_2 + \theta_3) \\ P'_z &= L_1 \cos\theta_1 + L_2 \cos\theta_1 \cos\theta_2 + L_3 \cos\theta_1 \cos(\theta_2 + \theta_3). \end{aligned}$$

Substituting for the known θ_1 and rearranging produces two equations in two unknowns of the form:

$$\begin{aligned} c &= a\cos(\theta_2 + \theta_3) + b\cos\theta_2 \\ d &= a\sin(\theta_2 + \theta_3) + b\sin\theta_2. \end{aligned}$$

Paul[2] shows the solution for θ_3 as:

$$\theta_3 = \text{a}\,tan\,2\left(\frac{\pm\sqrt{1-\left(\frac{c^2+d^2-a^2-b^2}{2ab}\right)^2}}{\frac{c^2+d^2-a^2-b^2}{2ab}}\right).$$

Substituting θ_3 into the forward position equations yields two equations in one unknown of the form:

$$\begin{aligned} g &= e\cos\theta_2 - f\sin\theta_2 \\ h &= e\sin\theta_2 + f\cos\theta_2. \end{aligned}$$

Wolovich[3] shows these equations have the solution:

$$\theta_2 = \text{a}\,tan\,2(eh - fg, eg + fh).$$

Again because θ_2, θ_3, and θ_4 are in parallel:

$$\theta_4 = \Phi - \theta_2 - \theta_3.$$

The remaining unknowns are θ_5 and θ_6. Because the axes of rotation for these angles intersect at a point, the following Euler angle extraction process at the point of intersection will find $\theta_{5\text{ and }6}$.

$$\begin{aligned} {}^0_6R &= R_y(\alpha)R_x(\beta)R_z(\gamma) \\ {}^0_4R &= R_x(-\theta_1)R_y(\Phi) \\ {}^4_6R &= {}^0_4R^{-1}\,{}^0_6R. \end{aligned}$$

Extracting YXZ Euler angles from ${}^4_6R$ completes the solution for θ_1 through θ_6.

III. INTELLIGENT ASSISTANCE

As the interaction between the operator and the machine begins to increase in sophistication, the level of control progresses from manual control to intelligent assistance. This section describes a kinematic configuration advisor implemented as an intelligent operator-assist interface. Through the assist interface, the operator establishes EEF locations for the robot's two arms. The computer algorithms underlying the interface then use a simulated annealing optimization algorithm to generate a small set of ranked configuration options that satisfy the constraints. The algorithms rank the options based on multiple performance criteria. The interface then presents

these options to the operator via a graphical computer interface.

The two EEF locations represent twelve equality constraints (six per EEF). The optimization algorithm tracks these constraints to reduce the solution space from seventeen DOF to five DOF. In other words, the algorithm only looks for optima within the robot's null-space (self-motion space). This technique, called constraint tracking, dramatically increases the speed of the optimization. The following discussion outlines the performance criteria, the constraint tracking algorithm, and the simulated annealing optimization.

A. Performance Criteria

Van Doren and Tesar[4] have formulated and implemented in software over 30 performance criteria. These criteria emphasize task-based performance indicators derived from the physical description of the manipulator. These formulations emphasize efficiency and portability. Available computing power makes decisions based on several of these criteria possible in real-time. Given the rapid pace of advancements in computational speed, it will soon be possible to employ the entire suite of performance criteria in a real-time decision making process. Table 2. lists the general categories of these performance criteria. Continuing work focuses on issues of normalization and multiple criteria fusion.

Table 2. General categories of performance criteria.

Category	Characteristics
constraint criteria	physical limitations
geometric	task independent
inertial	from dynamic models
compliance	design and operational issues
kinetic energy	content and distribution

Elementary physical limitations form the basis for the constraint criteria. These limitations restrict joint travels, joint speeds, joint accelerations, and joint torques. The joint travel availability is a representative criterion that seeks to keep the joint displacements as near as possible to the midpoints of their travel.

The Jacobian matrix forms the basis for the geometric performance criteria. These criteria are task independent and based only on the geometry of the robot, thus these criteria are formulated once for each robot with no need for reformulation if the task changes.[5]

The inertial performance criteria have their basis in dynamic models of forces and torques within the robot and are essential to the intelligent design and application of robots. The rate of change of inertial criteria measures how fast the robot can respond to torque and force demands. They are especially important because larger actuators or higher gear ratios can supply more torque, but both will slow the overall response of the robot to external disturbances.

The compliance criteria describe the robot's ability to perform precision operations under load. They also correspond to the vibratory modes of the robot. Of the compliance criteria, the potential energy partition values are particularly important. The potential energy partition values measure the distribution of compliance energy and how it changes as the robot moves. An unusually high compliance energy content in any part of the robot indicates a problem with the robot's design. Rapid changes in compliance energy indicate large local forces, which correspond to large actuator demands and decreased precision.

The kinetic energy performance criteria address high-level issues represented in relatively simply formulations. Large changes in kinetic energy correspond to very large demands on actuator power. Very rapid changes in the kinetic energy represent shocks to the robot.

B. Constraint Tracking

Constraint tracking uses the equality constraints on the position and orientation of the robot's EEF to reduce the solution space of the optimization problem by six (three position and three orientation). If the robot has two arms, then constraint tracking will reduce the solution space by twelve. Figure 3. depicts the geometry of the transformations.

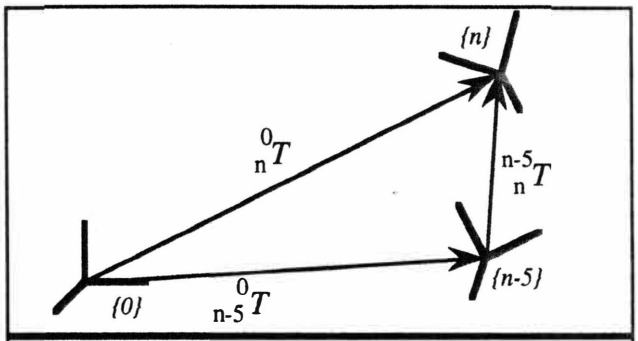

Figure 3. Transforms for constraint tracking

The implementation is straight-forward. Concatenating the geometric transformations associated with these equality constraints generates the transformation between the EEF frame and the robot's base frame:

$$^0_{EEF}T .$$

To satisfy the constraints, the transformation associated with the robot's n joints — $\theta_0 - \theta_n$ — must equal the above transformation:

$$ {}^{0}_{n}T = {}^{0}_{EEF}T . $$

Tracking the equality constraints requires extracting from ${}^{0}_{n}T$ a transform associated with only six joint displacements. The extraction procedure follows as:

$$ {}^{0}_{n}T = {}^{0}_{n-5}T \, {}^{n-5}_{n}T $$

and

$$ {}^{n-5}_{n}T = {}^{0}_{n-5}T^{-1} \, {}^{0}_{n}T . $$

Inverting the transform ${}^{n-5}_{n}T$ using inverse kinematics generates six joint displacements — $\theta_{n-5} - \theta_n$ — to satisfy the six equality constraints.

C. Simulated Annealing

The operator assist interface must solve a global optimization problem. Table 3. lists some options for finding global optima. These options include: a "shotgun" approach tracking gradients from different starting places, simulated annealing based on models of the physical annealing process, genetic algorithms based on models of biological genetics, brute force exhaustive evaluation, and the Monte Carlo based on randomness and statistics. All of these methods will solve global optimization problems. The difficulty lies in the need for interactive response (a few seconds) from the configuration advisor. In an optimization with seventeen DOF, none of these methods would have interactive response on available computer hardware. With constraint tracking, all of the methods except brute force will have interactive response in a configuration advisor application. This section discusses an implementation of the simulated annealing method. Even in complex environments with multiple obstacles and competing performance criteria, the implementation has proven reliable.

Table 3. Global Optimization Methods

Method	Basis
shotgun	gradient tracking
simulated annealing	probability distribution
genetic algorithms	genetics in biological systems
brute force	explicit evaluation of function
Monte Carlo	randomness and statistics

Annealing describes a process of heating a material to an elevated temperature and then cooling it slowly. The slow cooling allows the material to reach a low energy state in which it is ductile. With no intelligence or systematic strategy, some materials minimize energy state during the slow cooling. Simulated annealing models this process on a computer. The model is based on the Boltzmann probability distribution:

$$ \text{Prob}(E) \approx exp\left(-\frac{E}{kT}\right) $$

In this equation, E is the energy of the system, k is Boltzmann's constant, and T is the temperature. Essentially, Boltzmann states that a system's energy probabilistically distributes depending upon the temperature. As the temperature increases, the probability of the system assuming a higher energy state increases. As the temperature decreases, the probability of the system leaving a lower energy state decreases. Each configuration option corresponds to an energy state. Because simulated annealing algorithms sometimes leave lower energy states for higher ones, they can escape from local minima. Simulated annealing algorithms typically include a method of generating random changes in the system's configuration. The random changes represent trial configurations evaluated using the Boltzmann probability distribution. If the distribution indicates, the system assumes the trial configuration; otherwise it is discarded.

In the configuration advisor application, a single set of joint displacements $(\theta_0 - \theta_n)$ is one trial configuration. The algorithm generates the displacements for the redundant joints (five for the DAWM) randomly and then solves for the remaining joint displacements (twelve for the DAWM) using inverse kinematics. Performance criteria values associated with the trial configuration are the equivalent of energy in the algorithm. The example application calculates the energy as the weighted sum of two elementary criteria, though continuing work is investigating more sophisticated criteria fusion schemes. One of the criteria measures the approach to joint travel limits and the other criteria measures the approach to collisions. If the trial exceeds a travel limit or would result in a collision, the algorithm rejects the configuration immediately.

IV. SHARED CONTROL

There is a quantum leap in complexity as the interaction between operator and machine progresses from the level of intelligent assistance to the level of shared control. The coupled-Cartesian control mode is an example of shared control. A computer algorithm is automatically controlling extra kinematic resources. To reasonably deploy these resources, the computer algorithm needs a great deal of information about the task at hand and the robot's environment. The location of obstacles in the environment

is of primary importance. Implementing the coupled-Cartesian control mode for the DAWM requires a solution of the inverse kinematics problem in the redundant case. A number of researchers have developed and implemented solutions to this problem. Whitney[6] was quite influential with his resolved motion rate control that suggests the use of the pseudo-inverse to resolve redundancy. Liegeois[7] showed the extension of this method to include self-motions via the null-space. The coupled-Cartesian control mode implemented a solution based on direct constraint tracking and multicriteria optimization[8], though the concept of the control mode is generic with respect to the particular solution method.

V. CONCLUSIONS

A spectrum of tasks in unstructured environments characterizes the D&D mission. Telemanipulators represent a technology for accomplishing a portion of the mission's task spectrum. Giving these telemanipulators extra kinematic resources enables them to perform a wider range of tasks, thus further amortizing costs. The extra kinematic freedom also poses new user interface questions because the operator must now control a more complex system.

This paper developed five control modes for telemanipulators with extra kinematic resources. The modes fall into the categories of manual control, intelligent assistance, and shared control. All five control modes have been implemented and tested on actual telemanipulator hardware. The manual control modes could be applied immediately to D&D tasks. Implementing the shared control modes in actual D&D tasks requires supplying the computer with reliable data describing the telemanipulator's environment. Clearly, the location of obstacles is of primary importance. Intelligent assistance falls between shared and manual control. This mode is useful when there is some information about the location of obstacles, but the information is either limited or not guaranteed reliable.

Testing of the algorithms included computer simulation for the DAWM and hardware implementation in mock D&D tasks with another dual-arm robot having 17 DOF. This paper described a number of the implementation details. Notable among these details is a closed-form reverse position analysis for the Schilling manipulator geometry. Though the Schilling geometry does not include a spherical wrist, the analysis requires solving only second-order polynomials. Other notable details include the geometric transformations for a constraint-tracking technique that dramatically improves the solution speed of the shared control algorithms.

The testing revealed the efficiency of the control mode depends upon the task at hand. Joint control is best for extricating the robot from difficult configurations, but is not suitable for precisely controlling the robot's EEF. Decoupled-Cartesian is a general-purpose mode best suited for material transport and tool deployment. The self-motion mode allows for some optimization and is a useful extension of decoupled-Cartesian control. These first three modes are useful when there is no reliable information about the exact location of obstacles. The advisor mode is useful when there is limited information about the location of obstacles. The coupled-Cartesian is the most efficient mode in terms of task performance, but requires extensive and reliable information about the robot's environment.

REFERENCES

1. J. V. Draper, "Teleoperators for Advanced Manufacturing: Applications and Human Factors Challenges," *The Inter. Journal of Human Factors in Manufacturing,* Vol. 5, No. 1, pp 53-85 (1995).

2. R. Paul, *Robot Manipulators: Mathematics, Programming, and Control*, The MIT Press, Cambridge (1981).

3. W. Wolovich, *Robotics, Basic Analysis and Design*, CBS College Publishing, New York (1987).

4. M. J. Van Doren, and D. Tesar, "Criteria Development to Support Decision Making Software for Modular, Reconfigurable Robotic Manipulators," Report to the U.S. Department of Energy under Grant No. DE-FG-02-86NE37966.

5. K. Cleary, and D. Tesar, "Incorporating Multiple Criteria in the Operation of Redundant Manipulators," *Proceedings, 1990 IEEE International Conference on Robotics and Automation*, Vol. 1, pp. 618-623 (1990).

6 Whitney, D. E., 1969, "Resolved Motion Rate Control of Manipulators and Human Prostheses," *IEEE Transactions on Man-Machine Systems*, Vol. MMS-10, No. 2, pp. 47-53.

7 A. Liegeois, "Automatic Supervisory Control of the Configuration and Behavior of Multibody Mechanisms," *IEEE Transactions on Systems, Man, and Cybernetics*, Vol. SMC-7, No. 12, pp. 868-871 (1977).

8 R. Hooper and D. Tesar, "Motion Coordination Based on Multiple Performance Criteria with a Hyper-Redundant Serial Robot Example," *Proceedings of the 10th IEEE International Symposium on Intelligent Control,* pp.133-138 (1995).